Microstructure and properties of giant magneto-resistant Au80Co20, Au80Co10Fe10, Cu70Ni25Fe4Mn and Cu53Ni31Fe15Mn

Kooi, B.J.; Vystavel, T.; de Hosson, J.T.M.

Published in:
Scripta Materialia

DOI:
10.1016/S1359-6462(01)00848-X

Publication date:
2001

PERGAMON

Scripta mater. 44 (2001) 1461–1464

Scripta MATERIALIA

www.elsevier.com/locate/scriptamat

MICROSTRUCTURE AND PROPERTIES OF GIANT MAGNETO-RESISTANT $Au_{80}Co_{20}$, $Au_{80}Co_{10}Fe_{10}$, $Cu_{70}Ni_{25}Fe_4Mn$ AND $Cu_{53}Ni_{31}Fe_{15}Mn$

B.J. Kooi, T. Vystavel and J.Th.M. De Hosson

Department of Applied Physics, Materials Science Centre and Netherlands Institute for Metals Research, University of Groningen, Nijenborgh 4, 9747 AG Groningen, The Netherlands

(Received August 22, 2000)
(Accepted in revised form December 27, 2000)

Keywords: Transmission electron microscopy; Giant magneto-resistance; Alloys; Annealing

Introduction

The past decade a vast amount of studies were devoted to Giant-Magneto-Resistive (GMR) materials. Most materials investigated were composed of a multi-layered structure, but also granular systems received a lot of attention. The general concept of most studies consisted of a combination of magneto-resistance and magnetization measurements for various temperatures in-between liquid He and room temperature to characterize the materials synthesized. Most micro-structural characteristics were deduced from the magnetization measurements and only scarcely a single (HR)TEM image was added to the work. The starting point of our work is the investigation of the microstructure of the materials by means of HRTEM and Analytical TEM (ATEM).

Metallurgical routes for producing GMR materials have two main advantages over the commonly used sputter-deposition methods: (i) it is a more easy and a much cheaper route to produce large quantities of material due to its self-assembling nature and (ii) bulk GMR materials are obtained instead of only thin films. Of course also clear disadvantages exist of which probably the most dominant one is the large magnetic field needed to induce significant GMR effects. From a more fundamental point of view metallurgical routes are of interest for GMR since a wide variety of structures can be prepared: magnetic precipitates can be formed in a non-magnetic matrix by either nucleation and growth or by spinodal decomposition. Such precipitates have a certain shape, an average size, a size distribution and a distribution in separation distance between neighboring precipitates. The interfaces between the particles and the matrix can be either sharp or diffuse (in case of spinodal decomposition) and such interfaces can be coherent, semi-coherent or incoherent. All these factors may influence GMR, but not much fundamental knowledge of the precise role they play is available. A second interesting micro-structural feature occurs if the composition of the alloy is changed such that the magnetic phase is brought from below to above the percolation limit.

Up to now we studied 4 alloys: $Au_{80}Co_{20}$, $Au_{80}Co_{10}Fe_{10}$, $Cu_{70}Ni_{25}Fe_4Mn$, $Cu_{53}Ni_{31}Fe_{15}Mn$. The first 3 are below and the 4^{th} alloy is above the percolation limit of the magnetic phase. The last two alloys are known to exhibit spinodal decomposition where the last one will show decomposition waves along the $<100>$ crystal directions [1]. If in a single crystal this wave can be directed along only one of the $<100>$ (e.g. by applying a uniaxial strain) a bulk multi-layered structure is prepared by self-assembly. In the present paper some selected results obtained for the 4 alloys will be presented.

PII: S1359-6462(00)00848-X

Experimental

An arc furnace was used to prepare basic alloys from their pure components. The buttons were homogenized and cold-rolled to thin foils (thickness between 20 and 100 μm). Solid-solution annealing with subsequent water-quenching was used to arrive at alloys showing least decomposition of the magnetic and non-magnetic phase as possible. For the $Au_{80}Co_{20}$ alloy it was shown that this procedure was superior to melt spinning [2]. Finally, with heat treatments at relative low temperatures the decomposition between the magnetic and non-magnetic phase was invoked leading to suitable nano-structures.

For HRTEM and ATEM a JEOL 4000 EX/II and a JEOL 2010F equipped with X-Ray Energy Dispersive Spectrometry and a Gatan Imaging Filter were used, respectively. To control the GMR measurements a Quantum Design Physical Property Measurement System (PPMS) Q-6000 was used. An AC Resistance Bridge by Linear Research LR-700 was used to determine by a 4-point probe technique the resistance of the samples at 10, 100 and 300 K for magnetic fields up to 50 kOe. Some magnetization measurements were performed under the same conditions with a Quantum Design Magnetic Property Measurement System (MPMS). It consists of a second-order gradiometer employing a SQUID.

Results and Discussion

The microstructure of the $Au_{80}Co_{20}$ and $Au_{80}Co_{10}Fe_{10}$ alloys exhibits an interesting evolution as a function of the final heat treatments performed as was observed by HRTEM. After quenching coherent Co clusters with a maximum size of about 4 nm and with a tendency to have a truncated octahedral shape are observed in $Au_{80}Co_{20}$ [2]. During heating at 573 and 673 K these Co clusters grow significantly, loose their coherency (observable by the presence of Moiré) and most interestingly exhibit diffuse interfaces with the Au matrix [2]. This last observation indicates that in the Au-Co a spinodal decomposition occurs in agreement with the prediction given in [3]. At 773 K again sharp Co-Au interfaces were observed probably indicating that this temperature is above the locus of the spinodal. In all cases the Co has the fcc phase. Replacing 10 at.% Co in $Au_{80}Co_{20}$ by Fe has a dramatic influence on the evolution of the micro-structure. After annealing at 573 and 673 K no signs of spinodal decomposition are present anymore, just classical nucleation and growth occur. Moreover the precipitates, instead of having the fcc phase, obtain a bcc phase. For such small precipitates in the fcc Au matrix this change of phase totally alters the orientation relation and interface orientation between precipitate and matrix. A parallel topotaxy occurs for fcc Co and fcc Au where the interfaces have the tendency to be parallel to {111} and to lesser extent to {200}. An HRTEM image of a part of a bcc CoFe plate in the Au matrix as observed along a $<110>$ of Au as developed after annealing 24 hrs at 673 K is shown in Fig. 1. A Bain orientation relation holds between the precipitates and matrix where the main facets of the plates correspond to a 45° 'twisted' parallel {100} of Au and FeCo. The thickness of the plates is typically 4 nm. Fig. 2 shows the results of energy-filtering TEM applying a 3-window technique to the Fe and Co $L_{2,3}$ edges. The 4nm thick FeCo plates as viewed along the Au$<110>$ zone axis can be readily discerned. For this viewing direction only 1/3 of the plates is statistically observed edge-on; the other 2/3 is inclined $\pm 45°$. XEDS indicated that the Fe/Co ratio is nearly 1 in the precipitates and that the concentration of Fe and Co in the Au matrix is below 1 at.%. For Fe this is remarkable, because the solubility of Fe in Au at 673 K for the binary system is still about 10 at.%. The solubility of Co in Au at 673 K is very low. Apparently Co is efficient in dragging Fe out of its solution in Au.

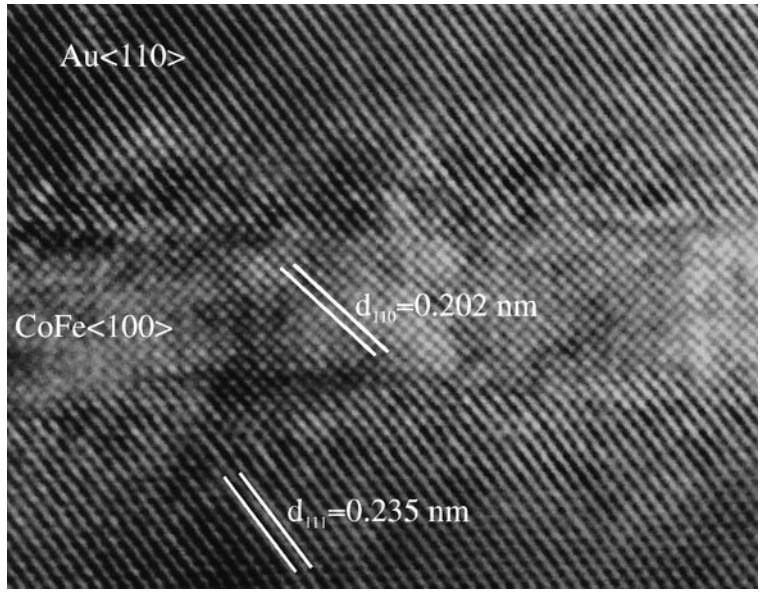

Figure 1. HRTEM image of a part of an edge-on observed bcc FeCo plate in an fcc Au matrix as observed along the Au<110> direction. The plates after solid-solution annealing, water quenching and annealing at 400 °C have a typical thickness of 4 nm and length of 25 nm.

Some characteristic data extracted from the MR curves we obtained as a function of the external magnetic field for 3 different alloys are listed in Table 1. For the first two alloys in Table 1, i.e those containing nano-sized magnetic precipitates the MR curves are to a large extent straightforward. If all precipitates are super-paramagnetic (and do not mutually interact) the MR curves are proportional to the M^2, with M the induced magnetization of the alloy [4]. If part of the magnetic precipitates become blocked, (ferro-magnetic) which can occur for increasing precipitate size or decreasing temperature also a linear dependence of MR on M is introduced [5]. Because in these granular systems a distribution of particles sizes occurs, super-paramagnetic and blocked particles will co-exist and both the linear and quadratic dependence arise [5]. In accordance we observed that the lower the measuring temperature the

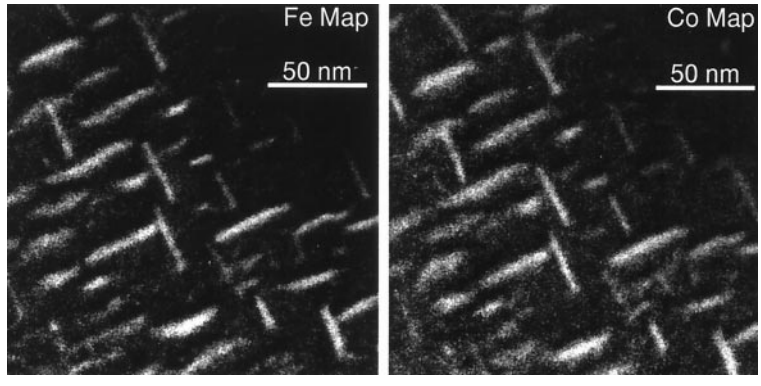

Figure 2. Energy-filtered TEM (GIF) images of bcc FeCo plates in a Au matrix as viewed along Au<110>. 1/3 of the plates with thickness of typically 4 nm are edge-on and 2/3 are inclined ±45°. The Fe and Co maps are obtained by using a 3-window technique to the Fe and Co $L_{2,3}$ edges.

TABLE 1
Size of the GMR Effect Defined by $\rho(0)$-$\rho(H)/\rho(0)$ for the Different Alloys and Annealing Conditions at Measuring Temperatures of 10 and 300 K and 5 and 50 kOe External Magnetic-Field Strength

		GMR at 10 K		GMR at 300 K	
Material	Heat treatment	5 kOe	50 kOe	5 kOe	50 kOe
$Au_{80}Co_{20}$	As-quenched	6.5%	29%	0.03%	1.7%
	1 hour at 573 K	10%	15%	—	—
	1 hour at 673 K	6.1%	8.7%	2.4%	3.2%
	1 hour at 773 K	1.9%	3.7%	0.96%	1.4%
$Cu_{70}Ni_{25}Fe_4Mn$	As-quenched	5%	13%	0.01%	0.7%
	30 min at 873 K	1.9%	6.8%	0.25%	0.6%
	2 hours at 873 K	1.2%	5.6%	0.20%	0.3%
$Cu_{53}Ni_{31}Fe_{15}Mn$	As-quenched	0.7%	2.1%	0.2%	2.7%
	19 min at 973 K	0.7%	5.6%	0.3%	1.1%
	5 hours at 973 K	1.4%	4.7%	0.4%	1.0%

higher the GMR effect. Annealing the as-quenched alloys increased in general the GMR effect for small magnetic fields (5 kOe). For large magnetic fields (50 kOe) annealing does only increase the GMR effect at 300 K not at 100 and 10 K. The MR curves for $Cu_{53}Ni_{31}Fe_{15}Mn$ with the magnetic phase above the percolation limit show more complex and less well understood behavior. Opposite to the systems without percolation the GMR effect of the as-quenched alloy now increases with increasing temperature for fields higher than 5 kOe. The origin of this behavior is electron scattering on magnetic fluctuations giving rise to a maximum MR around the Curie-temperature [6]. Because this as-quenched alloy has a T_C above room temperature [1] the GMR effect increases for increasing temperature as observed. In Ref.6 a nice overview is given of the influence on the MR curves of changing the magnetic content from below to above the percolation limit. For the annealed $Cu_{53}Ni_{31}Fe_{15}Mn$ alloy the behavior we observed becomes largely similar as for the systems containing precipitates. This is remarkable since the magnetic FeNi-rich phase still gives the appearance in the TEM images to be largely connected throughout the matrix grains. Apparently the magnetization becomes sufficiently independent in different parts of this network to give rise to the resembling behavior.

References

1. E. P. Butler and G. Thomas, Acta Metall. 18, 347 (1970).
2. H. Vrenken, B. J. Kooi, and J. Th. M. De Hosson, J. Appl. Phys. in press.
3. A. Hütten, J. Bernardi, S. Friedrichs, and G. Thomas, Scripta Metall. 33, 1647 (1995).
4. J. Q. Xiao, J. S. Jiang, and C. L. Chien, Phys. Rev. Lett. 68, 3749 (1992).
5. N. Wiser, J. Magn. Magn. Mater. 159, 119 (1996).
6. B. Dieny, et al., J. Magn. Magn. Mater. 126, 433 (1993).